SIMULATION OF LIQUID RESIN INFUSION PROCESS BY FINITE ELEMENT METHOD

A. Dereims[1,2,*], R. Troian[2], S. Drapier[2], J-M. Bergheau[3], P. de Luca[4]

[1]*ESI Group, Le Récamier, 70 rue Robert, 69458 Lyon Cedex 6, France.*
[2]*Claude Goux Laboratory (UMR CNRS 5146), Structure and Material Science Center, École Nationale des Mines de Saint-Étienne, 158 cours Fauriel, 42023 Saint-Étienne CEDEX 2.*
[3]*Laboratory of Tribology and Systems Dynamic (UMR CNRS 5513), University of Lyon, École Nationale d'Ingénieur de Saint-Étienne, 59 rue Jean Parrot, 42023 Saint-Étienne CEDEX 2, France.*
[4]*ESI Group, Aero Business Center - Aeroparc, 25 Rue Marcel Issartier, BP 20005, 33700 Mérignac, France.*
**arnaud.dereims@esi-group.com*

Keywords: Infusion, Post-filling, Stokes, Darcy

Abstract
Infusion processes are a cheaper alternative to the usual injection process to realize big composite parts. However the bad control of the final properties of the molded part is a disincentive to their democratization at industrial level. We are presenting an advanced modeling method, coupling fluid flows with finite deformation solid mechanics, in order to anticipate as best as possible thickness variation of the part and infusion time.

1 Introduction

Composite manufacturing processes by resin infusion have been developed for years to bring a cheaper solution to big parts production. Those processes allow a significant cost reduction in raw materials storage and mold fabrication, a shorter infusion time and limit void formation. However, the lack of control on the final properties of the part, implying long and expensive process settings, significantly reduce the above-mentioned advantages. So we are proposing a full model so simulate the liquid resin infusion process, in order, to anticipate the potential problems numerically.

2 Liquid Resin Infusion process description

Liquid Resin Infusion (LRI) is among the most used infusion process in industrial application. It consists of creating a liquid film of resin, on the top of the dry preforms, thanks to a very permeable material, the distribution medium. Then, it is the pressure differential between the vent (0 bar) and the injection line (atmospheric pressure) that provokes the infusion of the resin in the thickness direction (figure 1a). Finally, a pressure and temperature cycle is applied to the system to bring the resin in a solid state. The flexibility of the vacuum bag does not allow maintaining a constant thickness during the whole process, while its good control is mandatory in the geometrical and mechanical properties of the final part.

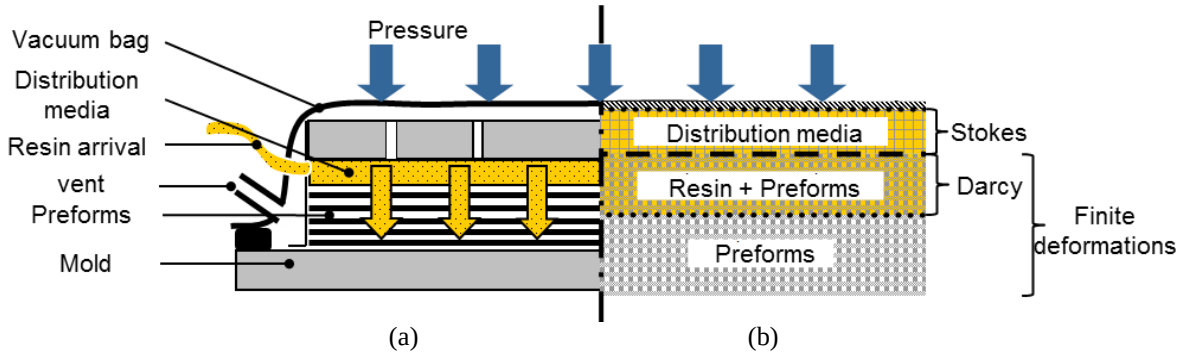

Figure 1. (a) Principle of the Liquid Resin Infusion process (LRI). (b) Proposed model [1]

3 Modeling and numerical aspect

The chosen model is the one proposed by P. Celle in his PhD thesis [1-2]. This innovative model, which particularity is the distribution medium modeling, is based on spatial and time decomposition. Spatially the system is divided in three zones (Figure 1b):

- Stokes zone: fast flow zone constituted of the distribution medium and the resin,
- Darcy zone: incompressible flow of the resin in the preforms submitted to finite deformations,
- Dry preforms zone: zone constituted of non-impregnated preforms submitted to finite strains.

Four time periods corresponding to change in boundary conditions or physical problem can be identified:

- Pre-filling: initial compaction of the preforms due to the vacuuming of the system,
- Filling,
- Post-filling: re-compaction or "rest period" ending by the mechanical equilibrium mandatory to the dimensional quality of the final part,
- Curing (not studied here).

We will now describe the physical problems and the numerical tool used to solve them.

3.1 Pre-filling simulation: Solid mechanics in finite deformations

During the pre-filling stage, there is no resin in the system, so only the dry preforms zone need to be considered. At this stage, since vacuum is established in the mold, preforms are submitted to atmospheric pressure (1 bar) resulting in deformations. Neglecting volume forces we can write the momentum conservation equation as follow:

$$\mathrm{div}\underline{\underline{\sigma}} = \underline{f^s} \tag{1}$$

where $\bar{\bar{\sigma}}$ the overall constrain and $\overrightarrow{f_s}$ the contact forces. In addition, preforms are represented by an equivalent homogenous medium composed of rigid fibers, so that each macroscopic strain is reflected by fiber rearrangements at microscopic scale. This approach allows computing directly porosity from deformations with no need to use semi-empiric laws, expressing porosity or thickness variation as a function of pressure, as it is usually done in literature [3-4].

Numerically, the solid mechanics problem is non-linear on two counts, first due to the non-linear response of the preforms and second due to the finite deformations. Hyper-elasticity is treated by Newton-Raphson algorithm and finite deformations are treated by a quasi-static approach consisting in applying the global constrain by successive load step. We chose an updated lagrangian formulation in displacement (2):

$$\begin{cases} \forall\, \underline{\delta u}, \\ \int_{{}^{t}\Omega} {}^{t+\Delta t}_{t}\underline{\underline{S}} : {}^{t+\Delta t}_{t}\underline{\underline{\delta E}}\, dv - \int_{\partial^{t+\Delta t}\Omega_f} {}^{t+\Delta t}\underline{f}^{s} \cdot \underline{\delta u}^{t+\Delta t} ds = 0 \\ \underline{\underline{\sigma}} \cdot \underline{n} = {}^{t+\Delta t}\underline{f}^{s}, sur\ \partial\Omega_f \\ \underline{\delta u} \in E_{\underline{\delta u}} = \left\{ \underline{\delta u} \in\ H^1(\Omega) \,/\, \underline{\delta u} = \underline{0} \text{ sur } \partial\Omega_{\underline{u}} \right\} \\ \underline{u} \in E_{\underline{u}} = \left\{ \underline{u} \in\ H^1(\Omega) \,/\, \underline{u} = \underline{u}^{d} \text{ sur } \partial\Omega_{\vec{u}} \right\} \end{cases} \quad (2)$$

where $\underline{\underline{S}}$ is the second Piola-Kirchoff stress tensor, $\underline{\underline{\delta E}}$ is the virtual Green-Lagrange tensor, $\underline{f}^{s}$ are the contact forces and $\underline{\delta u}$ is the virtual displacement field.

3.2 Filling simulation: Resin flow

As described above, resin flows in a distribution media then preforms are infused under the vacuum action. In the so called stokes zone, the high permeability, allow us to consider, in a first approximation, an incompressible flow governed by stokes equation (3):

$$\begin{cases} \text{div}\left(2\mu \underline{\underline{D}}(\underline{v})\right) - \underline{\nabla} p = 0 \\ \text{div}\, \underline{v} = 0 \end{cases} \quad (3)$$

where μ is the resin viscosity, $\underline{\boldsymbol{v}}$ the resin velocity, p the resin pressure and $\underline{\underline{D}}(\underline{v}) = \frac{1}{2}\left(\underline{\underline{\nabla}} v + \underline{\underline{\nabla}}^{T} v\right)$ the eulerian strain rate associated to the velocity field $\underline{\boldsymbol{v}}$. While in the Darcy zone, we consider a Newtonian incompressible fluid flowing in low permeability (less than 10^{-9} m²) porous media governed by Darcy law (4):

$$\begin{cases} \underline{v} = \frac{1}{\mu} \underline{\underline{K}} \left(-\underline{\nabla} p + \rho \underline{g} \right) \\ \text{div}\, \underline{v} = 0 \end{cases} \quad (4)$$

where $\underline{\boldsymbol{v}}$ is the Darcy velocity or the macroscopic mean velocity of the resin with respect to the preforms, p the pore pressure, $\underline{\underline{K}}$ the permeability tensor, μ the resin viscosity and ρ volumetric mass of the resin.

From a numerical point of view, even if Darcy equation's form allow to solve separately pressure and velocity fields, in order to be consistent with the Stokes problem for the coupling, we chose to solve a mixed velocity/pressure formulation described in equations (5) and (6) with the finite element method stabilized by the mini element P1+/P1 [2]. The mini element P1+/P1 stand on the enrichment of the velocity field approximation by the introduction of an extra node in the center of the element (figure 2). Since the velocity field

degree of interpolation is higher than the pressure one, the Brezzi-Babuska condition is respected avoiding pressure parasite modes [5].

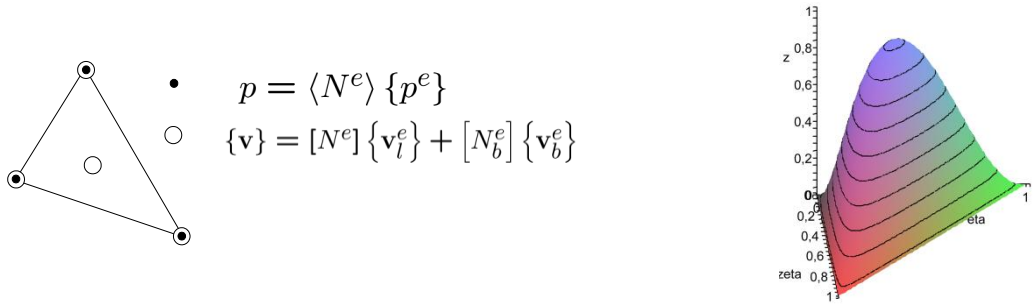

(a) (b)

Figure 2 : Mini-element P1+/P1 : (a) 2D triangle element, (b) form function associated to the extra node [1,2]

The dual mixed velocity/pressure formulation of Stokes problem:

$$\begin{cases} \forall \underline{\delta v}, \forall \delta P, \\ \int_\Omega 2\mu \underline{\underline{D}}(\underline{\delta v}) : \underline{\underline{D}}(\underline{v}) dv - \int_\Omega p \, \mathrm{div}\underline{\delta v} \, dv = \underbrace{\int_{\Omega_s} 2\mu \underline{\delta v} \underline{\underline{D}}(\underline{v}) \underline{n} ds - \int_{\Omega_s} \underline{\delta v} \, p \, \underline{n} ds}_{\int_{\Omega_s} \underline{\delta v} \cdot \underline{\underline{\sigma}} \cdot \underline{n} ds} \\ \int_\Omega \delta p \, \mathrm{div} \, \underline{v} \, dv = 0 \\ \underline{\delta v} \in E_{\underline{\delta v}} = \{\underline{\delta v} \in H^1(\Omega) \,/\, \underline{\delta v} = \underline{0} \text{ sur } \partial\Omega_{\underline{v}}\} \\ \underline{v} \in E_{\underline{v}} = \{\underline{v} \in H^1(\Omega) \,/\, \underline{v} = \underline{v_d} \text{ sur } \partial\Omega_{\underline{v}}\} \\ \delta p \in L^2(\Omega) \\ p \in L^2(\Omega) \end{cases} \quad (5)$$

The primal mixed velocity/pressure formulation of Darcy law :

$$\begin{cases} \forall \underline{\delta v}, \forall \delta P, \\ \int_\Omega \underline{\delta v} \, \underline{\underline{\frac{\mu}{K}}} \, \underline{v} \, dv + \int_\Omega \underline{\delta v} \, \underline{\nabla} p \, dv = \int_\Omega \underline{\delta v} \, \rho \, \underline{g} \, dv \\ \int_\Omega \underline{v} \, \underline{\nabla} \delta P \, dv = \int_\Omega \delta P \, \underline{v} \cdot \underline{n} \, ds \\ \delta P \in E_{\delta P} = \{\delta P \in H^1(\Omega) \,/\, \delta P = 0 \; sur \; \partial\Omega_P\} \\ p \in E_P = \{p \in H^1(\Omega) \,/\, p = p^d \; sur \; \partial\Omega_P\} \\ \underline{\delta v} \in L^2(\Omega) \\ \underline{v} \in L^2(\Omega) \end{cases} \quad (6)$$

3.2.1 Stokes / Darcy coupling method

The coupling between the two domains (Darcy and Stokes) is realized by considering the normal stress and normal velocity continuities across the interface and a controlled tangential velocity discontinuity. So, normal velocity ($\underline{v_d} \cdot \underline{n}$) on the interface taken into Darcy's domain is applied as boundary condition to stokes equations, and the hydrostatic pressure (p_s) taken

into stokes domain is applied to Darcy's law (figure 3). A new tangential velocity boundary condition is introduced, based on Beaver-Josef-Saffman condition, this condition consist of controlling the discontinuity on the interface with a drag coefficient (7):

$$\begin{cases} \underline{v_s} \cdot \underline{\tau} = -\frac{1}{\mu}\underline{\underline{K}}\left(\frac{\lambda^2 + 2\alpha\lambda}{1+\alpha\lambda}\right)\underline{\nabla p} \cdot \underline{\tau} \\ \lambda = \frac{H}{\sqrt{\underline{\underline{K}}}} \end{cases} \tag{7}$$

where H is the thickness of the fluid layer (Stokes domain), α the drag coefficient and $\underline{\tau}$ the unit tangent vector to the interface.

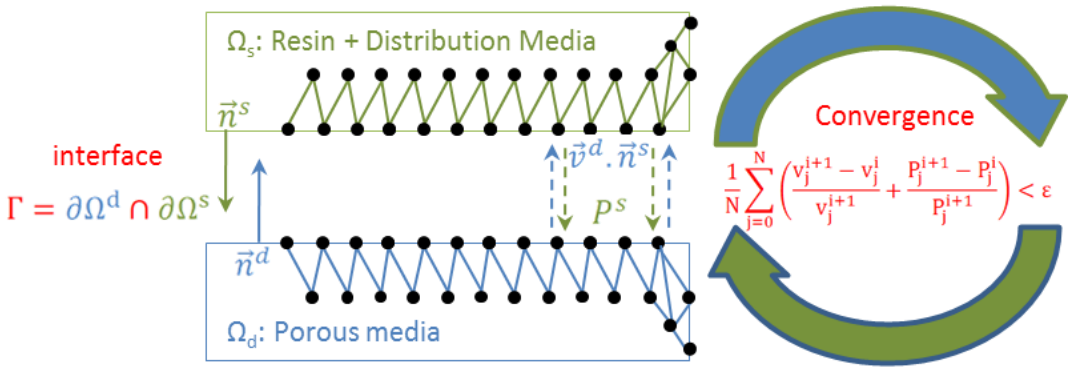

Figure 3: Stokes/Darcy coupling

Finally the problem is solved by an iterative method and the convergence checked by a relative error computed on velocity and pressure fields between two iterations.

3.2.2 Fluid / Structure coupling method

The fluid/structure strong coupling is treated iteratively in a quasi-static context (figure 4). Indeed, the Stokes/Darcy coupled problem is solved on fix grid (i.e. rigid preforms), the resin influence on the fibers being taken into account, through pore pressure by Terzaghi's law (8):

$$\overline{\overline{\sigma_{eff}}} = \overline{\overline{\sigma_{all}}} - \bar{\bar{I}}p \tag{8}$$

where $\overline{\overline{\sigma_{all}}}$ overall stress applied to the system, $\overline{\overline{\sigma_{eff}}}$ the effective stress in the fibers and $\bar{\bar{I}}$ the unity tensor. The non-linear mechanical problem in finite strain is, then, solved for a given pore pressure (*i.e.* for a Terzaghi equivalent behavior), finally, the strain influence is reflected by the porosity variation modifying the permeability ($\bar{\bar{K}}$) of the medium, determined with Karman-Cozeny law (9),

$$\bar{\bar{K}} = \frac{{d_f}^2}{16\overline{\overline{h_k}}}\frac{\emptyset^3}{(1-\emptyset)^2} \tag{9}$$

where d_f is the fiber diameter, h_k the Kozeny constant and $\emptyset$ the porosity. Finally, convergence is verified by a relative error computation on velocity and pressure fields of resin and solid displacement between two iterations.

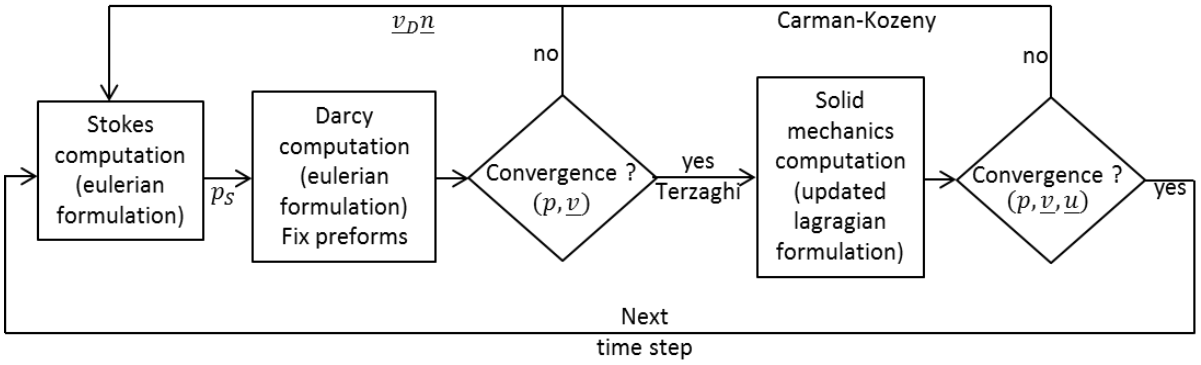

Figure 4: Stokes/Darcy/Solid mechanics coupling algorithm

3.3 Post-filling simulation: Unsteady Darcy flow

The filling stage is immediately followed by a stage, more or less long, of mechanical balancing, consisting, eventually, of a re-compaction of the system to reach the fiber fraction desired. To simulate this stage, referred as post-filling in literature [6], we introduced an unsteady Darcy equation (10) based on Brinkman equation.

$$\begin{cases} \dfrac{\rho}{\phi}\left(\dfrac{\partial \underline{v}}{\partial t} + \underline{v}\,\underline{\underline{\nabla v}}\right) + \underline{\underline{\dfrac{\mu}{K}}}\,\underline{v} = -\underline{\nabla} p + \rho \underline{g} \\ \operatorname{div} \underline{v} = 0 \end{cases} \tag{10}$$

4 Results and experimental validation

The above-described model has been implemented in the commercial C++ library Pro-Flot™[1] and then used to simulate various cases.

4.1 Experimental validation: simple plate

Simulation results were successfully compared to experiment in the case of a plate, during a first validation made by P. Wang [7]. This case was a plate measuring 335 mm x 335 mm, composed of 24 plies [90,0]. Initial thickness measured with a caliper was 9.8 mm. After initial compaction, a mean thickness of 6.18mm was measured, while the simulated one was 6.17 mm. After filling stage, simulated swelling was 0.63 mm when the experimental measure was 0.59 mm. Figure 5 shows initial conditions and some results.

[1] Finite element C++ library owned by Esi group (http://www.esi-group.com) base of PAM-RTM™.

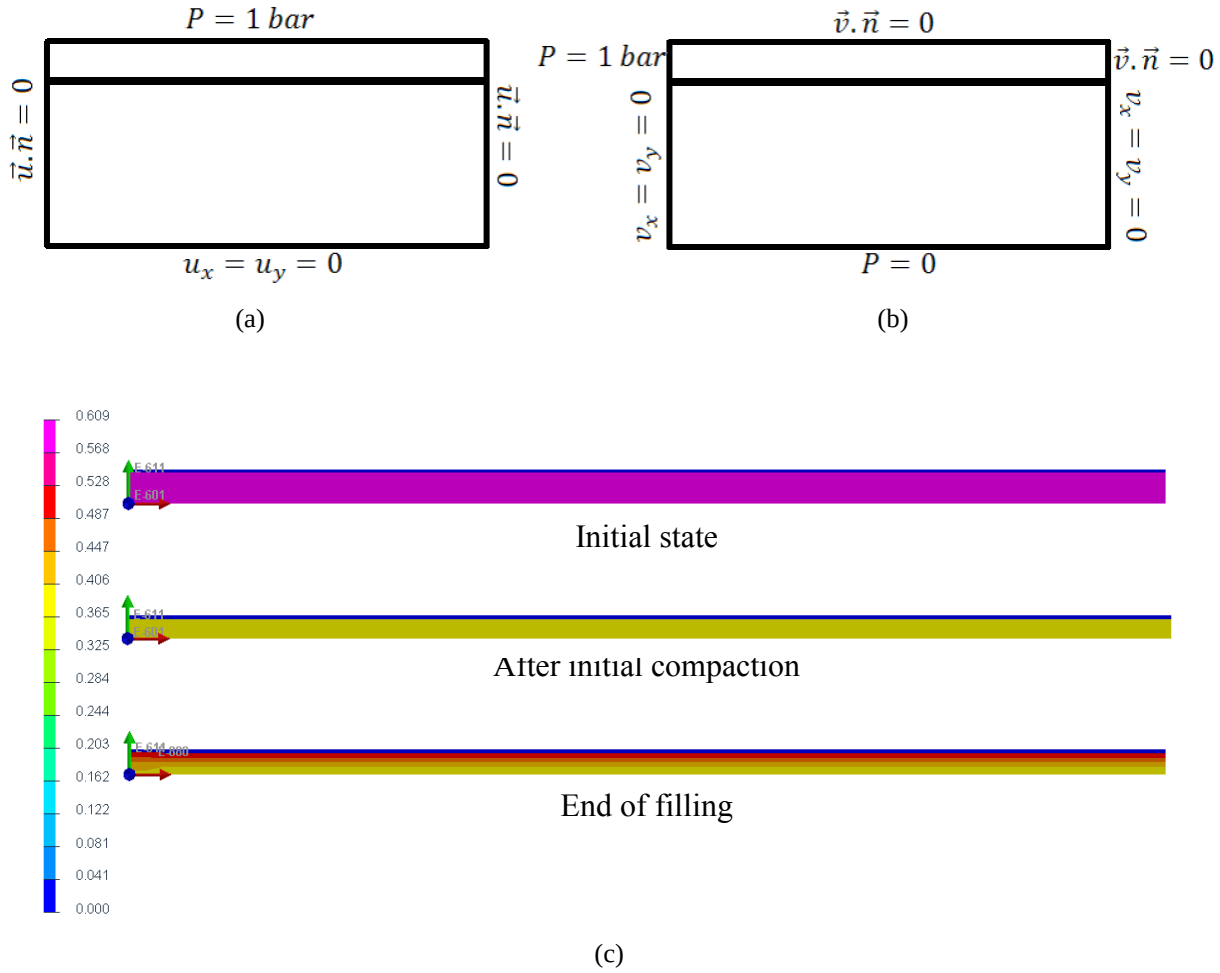

Figure 5: Simulation example: (a) Mechanical boundary conditions, (b) fluid boundary conditions , (c) Porosity field and geometry obtain after initial compaction and after filling stage

5 Conclusion

We presented an innovative model, by its global approach, to simulate fabrication process of composite parts by resin infusion. Caring about delivering to the professionals a simulation tool closer as possible to reality, we tried to consider the most of known phenomenon. To do that, we implemented a coupling method between Stokes, Darcy and solid mechanics equations which was compared successfully to experiment. However, this model needs other development to give results closer to the needs of industrials. Some improvements, as new thermal-chemical coupling, have been proposed and will be presented in future communications.

Acknowledgements

The authors would like to thanks the support of the European Union in the INFUCOMP project (European Community's Seventh Framework Program FP7/2009-2013 under grant agreement n°233926) financing partially these researches.

References

[1] Celle P., Drapier S., Bergheau J-M. Numerical modeling of liquid infusion into fibrous media undergoing compaction, *European Journal of Mechanics - A/Solids*, **27(4)**, pp 647-661 (2008).

[2] Celle P. Couplage fluide / milieu poreux en grandes déformations pour la modélisation des procédés d'élaboration par infusion, *PhD Thesis*, École Nationale des Mines de Saint-Étienne (2006).

[3] Gutowsky T., Morigaki T. The Consolidation of laminate composites, *Journal of Composite Materials*, **21(2)**, pp 172-188 (1987).

[4] Ouahbi T., Souad A., Bréard J., Ouagne P., Chatel S. Modeling of hydro-mechanical coupling in infusion processes, *Composites Part A : Applied Science and Manufacturing*, **38(7)**, pp 1646-1654 (2007).

[5] Arnold D.N., Brezzi F., Fortin M. A stable finite element for the Stokes equations, *Calcolo*, **21(4)**, pp 337-344 (1984).

[6] Šimáček P., Heider D., Gillespie Jr J.W., Advani S.G. Post-filling flow in vacuum assisted resin transfer molding processes: Theoretical analysis, *Composites Part A: Applied Science and Manufacturing*, **40(6-7)**, pp 913-924 (2009).

[7] Wang P., Drapier S., Molimard J., Vautrin A., Minni J-C. Characterization of Liquid Resin Infusion (LRI) filling by fringe pattern projection and in situ thermocouples, *Composites Part A: Applied Science and Manufacturing*, **41(1)**, pp 36-44 (2010).